M. Bergamasco, M. Lovera
Identification of Linear Models for the Dynamics of a Hovering Quadrotor
IEEE Transactions on Control Systems Technology, Vol. 22, N. 5, 2014, p. 1696-1707
doi:10.1109/TCST.2014.2299555

Identification of linear models for the dynamics of a hovering quadrotor

Marco Bergamasco, Marco Lovera*
Dipartimento di Elettronica, Informazione e Bioingegneria, Politecnico di Milano
Piazza Leonardo da Vinci 32
20133 Milano, Italy
email: {bergamasco, lovera}@elet.polimi.it

January 29, 2014

Abstract

Accurate dynamic modelling of helicopter aeromechanics is becoming increasingly important, as progressively stringent requirements are being imposed on rotorcraft control systems. System identification plays an important role as an effective approach to the problem of deriving or fine tuning mathematical models for purposes such as handling qualities assessment and control system design. In this paper the problem of deriving continuous-time models for the dynamics of a small-scale quadrotor helicopter is considered. More precisely, the continuous-time predictor-based subspace identification approach is adopted and the results obtained in an experimental study are presented and discussed.

1 Introduction

The quadrotor architecture is a very popular one for the development of rotorcraft UAV platforms (see, *e.g.*, [CLD05, BBS07] and the references therein), in view of its favorable dynamic characteristics (see [DSL09]): indeed, although they are frequently open-loop unstable, like most rotorcraft architectures, quadrotors exhibit a good degree of decoupling (*i.e.*, unlike conventional helicopters, acting on one of the controls essentially affects the corresponding degree of freedom only) which makes them easier to control. As discussed in, *e.g.*, [HMLO02, PM09, MK12] and the references therein, mathematical models for the dynamics of quadrotors are easy to establish as far the kinematics and dynamics of linear and angular motion are concerned. In fact a significant portion of the literature dealing with quadrotor control is based on such models, probably also because of the elegant mathematical methods which can be deployed to design feedback controller on this basis. Unfortunately, characterising aerodynamic effects and additional dynamics such as, *e.g.*, the response of the controlled speed of the individual rotors, is far from trivial, and has led to the development of many approaches to the experimental characterisation of the dynamic response of the quadrotor. Broadly speaking, two classes of methods to deal with this problem can be defined. The first

*Corresponding author

class of methods is based on the calibration of the parameters of detailed physical models, see for example [KT04, DMB06]. The second class of methods is based on a black-box identification approach and as such aims at extracting the information about the dynamics of the system directly (and solely) from measured input-output data (see for example [LCMK02, KCL06, HOBM08]). Note, in passing, that system identification has been known for a long time as a viable approach to the derivation of control-oriented dynamic models in the rotorcraft field (see for example the survey paper [HK97], the recent books [TR06, Jat06] and the references therein). Black-box identification of rotorcraft models leads to very specific requirements for identification methods: it is customary to work with continuous-time models, so that dedicated identification methods are needed; most rotorcraft vehicles are open-loop unstable, so that methods for closed-loop identification are desirable; data is collected in separate experiments for each input channel, so the capability to handle separate datasets is important; finally, the identification problem is a multivariable one. To our best knowledge, none of the above cited references provides methods compliant with all the above listed requirements.

In the system identification literature, on the other hand, one of the main novelties of the last two decades has been the development of Subspace Model Identification (SMI) methods (see, *e.g.*, [VODM96, VV07]), which have proved extremely successful in dealing with the estimation of state space models for multiple-input, multiple output (MIMO) systems. Surprisingly enough, until recently these methods have received limited attention from the rotorcraft community, with the partial exception of some contributions such as [VV94, BL97, Lov03]), which however rely on SMI methods assuming open-loop operation. SMI methods are particularly well suited for rotorcraft problems, for a number of reasons. First of all, the subspace approach can deal in a very natural way with MIMO problems; in addition, all the operations performed by subspace algorithms can be implemented with numerically stable and efficient tools from numerical linear algebra. Finally, information from separate data sets (such as generated during different flight experiments) can be merged in a very simple way into a single state space model. Recently, see [LI11], the interest in SMI for helicopter model identification has been somewhat revived and the performance of subspace methods has been demonstrated on flight test data. However, so far only methods and tools which go back 10 to 15 years in the SMI literature (such as the MOESP algorithm of [Ver94]) have been considered. Therefore, the further potential benefits offered by the latest developments in the field have not been fully exploited. Among other things, present-day approaches can provide unbiased model estimates from data generated during closed-loop operation, as is frequently the case in experiments for rotorcraft identification because

of open-loop instability (see, *e.g.*, [CP05, Chi07, HDQ05]) and the direct estimation of continuous-time models from (possibly non-uniformly) sampled input-output data (see [BL11b] and the references therein).

In view of the above discussion, the aim of this paper is to demonstrate by means of the experimental case study of a small-scale quadrotor helicopter the applicability of state-of-the-art SMI methods to the identification of rotorcraft flight dynamics. More precisely (see also the preliminary results presented in [BL11a, SBL12]), the continuous-time predictor-based subspace identification approach proposed in [BL11b] is applied to flight data collected during dedicated identification experiments and a model for the hovering quadrotor is derived. Particular emphasis is placed on the analysis of the uncertainty associated with the identified model, both in the frequency domain and in the time domain, which provides useful information in a control design perspective. To this purpose, the bootstrap approach to uncertainty analysis first proposed in [BL00] for discrete-time SMI is extended to the continuous-time case and applied to the quadrotor problem. To the best knowledge of the Authors this is the first contribution considering the application of a closed-loop identification method to the identification of a rotorcraft system and providing a detailed analysis of model uncertainty associated with flight experiments, with specific reference to the issues arising because of closed-loop operation.

The paper is organised as follows. Section 2 provides some background on the model identification technique considered in this paper and on the problem of assessing model uncertainty associated with the identified models. The experimental setup considered in this paper, as well as the approach followed in the identification and validation experiments are presented in Section 3. Finally, the results obtained in the estimation of linear models for the hovering quadrotor and in the analysis of their characteristics are presented in Section 4.

2 Approach

2.1 Requirements for quadrotor model identification

The identification of rotorcraft flight dynamics poses a number of challenges, which in turn give rise to very specific requirements in the choice of a suitable method. First of all, in the rotorcraft community (and, in general, in aerospace applications) it is customary to work with continuous-time models rather than with discrete-time ones, mainly because they are more intuitive, so that identification methods for continuous-time models are needed. In addition, rotorcraft systems tend to be open-loop unstable (in this respect the quadrotor is no exception and is quite representative), so that identification experiments have to be carried

out in closed-loop, either under feedback from a human operator or under automatic control (see, *e.g.*, [TR06] for a detailed discussion of the pros and cons of the two approaches), and a model identification method capable of providing unbiased estimates of the open-loop dynamics from data collected in closed-loop would be preferable. Furthermore, in view of both the open-loop instability and the complexity of some piloting tasks, data for identification are frequently collected in separate experiments in which each input channel is excited separately. The capability to handle easily such separate datasets in a single identification procedure is therefore desirable. Finally, even taking into account the fact that for a quadrotor the individual axes can be identified separately, the identification problem remains a multivariable one as typically more than one output variable per axis must be considered.

All the above discussed requirements have led to the choice of the adopted approach, as detailed in the following Section.

2.2 Continuous-time predictor-based subspace model identification

As is well known, SMI methods offer a simple way of dealing with multivariable identification problems, so they can take into account the last of the requirements listed in the previous Section. Similarly, dealing with data collected in multiple experiments is quite natural in the SMI framework as information from data is encoded in the form of algebraic equations (the so-called data equations), which can be stacked alongside each other regardless of the number of experiments in which the data have been collected. As for, respectively, the requirement to provide unbiased estimates from closed-loop data and the need for continuous-time models, the two issues have been tackled separately in a number of publications (see, *e.g.*, [LM96, CV97, CP05, Chi07, HDQ05] for closed-loop SMI and [JVC99, Hav01, OKY02, OK04, MOGG08] for continuous-time SMI) and more recently in a unified approach (see [BL11b]). In view of this discussion, the method proposed in the last cited reference has been adopted; a short overview of the key ideas is provided in the following.

Consider the linear, time-invariant continuous-time system

$$\begin{aligned} dx(t) &= Ax(t)dt + Bu(t)dt + dw(t),\ x(0) = x_0 \\ dz(t) &= Cx(t)dt + Du(t)dt + dv(t) \\ y(t)dt &= dz(t) \end{aligned} \tag{1}$$

where $x \in \mathbb{R}^n$, $u \in \mathbb{R}^m$ and $y \in \mathbb{R}^p$ are, respectively, the state, input and output vectors and $w \in \mathbb{R}^n$ and $v \in \mathbb{R}^p$

are the process and the measurement noise, respectively, modelled as Wiener processes with incremental covariance given by

$$E\left\{\begin{bmatrix} dw(t) \\ dv(t) \end{bmatrix}\begin{bmatrix} dw(t) \\ dv(t) \end{bmatrix}^T\right\} = \begin{bmatrix} Q & S \\ S^T & R \end{bmatrix} dt.$$

The system matrices A, B, C and D, of appropriate dimensions, are such that (A,C) is observable and $(A,[B,Q^{1/2}])$ is controllable. Assume that a dataset $\{u(t_i),y(t_i)\}$, $i \in [1,N]$ of sampled input/output data (possibly associated with a non equidistant sequence of sampling instants) obtained from system (1) is available. Then, the problem is to provide a consistent estimate of the state space matrices A, B, C and D (up to a similarity transformation) on the basis of the available data. Note that unlike most identification techniques, in this setting incorrelation between u and w,v is not required, so that this approach is viable also for systems operating under feedback.

Consider the family of Laguerre filters, defined as

$$\mathscr{L}_i(s) = \sqrt{2a}\frac{(s-a)^i}{(s+a)^{i+1}} \tag{2}$$

and denote with $\ell_i(t)$ the impulse response of the i-th Laguerre filter. Then, it can be shown that the set $\{\ell_0,\ell_1,\ldots,\ell_i,\ldots\}$ is an orthonormal basis of $\mathscr{L}_2(0,\infty)$. The continuous-time algorithm employed in this paper is based on the results first presented in [OK04, Oht05], and further expanded in [KO10, Oht11a, Oht11b], which allow to obtain a discrete-time equivalent model starting from the continuous-time system (1), along the following lines. Under the stated assumptions, system (1) can be written in innovation form as

$$\begin{aligned} dx(t) &= Ax(t)dt + Bu(t)dt + Kde(t) \\ dz(t) &= Cx(t)dt + Du(t)dt + de(t) \\ y(t)dt &= dz(t). \end{aligned} \tag{3}$$

Considering now the sequence of sampling instants t_i, $i = 1,\ldots,N$, the input u, the output y and the innovation e of (3) are subjected to the transformations

$$\tilde{u}_i(k) = \int_0^\infty \ell_k(\tau)u(t_i+\tau)d\tau, \quad \tilde{y}_i(k) = \int_0^\infty \ell_k(\tau)y(t_i+\tau)d\tau, \quad \tilde{e}_i(k) = \int_0^\infty \ell_k(\tau)de(t_i+\tau)d\tau \tag{4}$$

where $\tilde{u}_i(k) \in \mathbb{R}^m$, $\tilde{e}_i(k) \in \mathbb{R}^p$ and $\tilde{y}_i(k) \in \mathbb{R}^p$. Then the transformed system has the state space representa-

tion

$$\xi_i(k+1) = A_o\xi_i(k) + B_o\tilde{u}_i(k) + K_o\tilde{e}_i(k),\ \xi_i(0) = x(t_i)$$
$$\tilde{y}_i(k) = C_o\xi_i(k) + D_o\tilde{u}_i(k) + \tilde{e}_i(k) \tag{5}$$

where the state space matrices are given by

$$A_o = (A-aI)^{-1}(A+aI), \quad B_o = \sqrt{2a}(A-aI)^{-1}B, \quad K_o = \sqrt{2a}(A-aI)^{-1}K \tag{6}$$
$$C_o = -\sqrt{2a}C(A-aI)^{-1}, \quad D_o = D - C(A-aI)^{-1}B.$$

From this point on, one can turn to the problem of estimating A_o, B_o, C_o and D_o in the discrete-time model (5), which is a *bona fide* discrete model identification problem (even though index k does not refer to time sampling but rather to projection onto $\ell_k(t)$), to which SMI algorithms for discrete-time identification can be applied. Once estimates for A_o, B_o, C_o and D_o have been worked out, it is possible to recover estimates for the continuous-time state space matrices A, B, C and D by inverting the bilinear (and, therefore, well posed) transformations (6). In view of the requirement to operate with data generated under feedback, the discrete-time PBSID$_{opt}$ SMI method proposed in [Chi07] is employed for the estimation of A_o, B_o, C_o and D_o, which can guarantee unbiasedness of the estimates even when the input u and the noise processes w and v are correlated. A detailed description of the algorithm is omitted for brevity, the interested reader can check either [BL11b] for a complete presentation of the continuous-time version of PBSID$_{opt}$ or [Chi07] for the original discrete-time formulation.

2.3 Quantifying model uncertainty: a bootstrap-based approach

For the purpose of control design it is desirable to have information about the reliability of the identified model. In this Section a procedure for the evaluation of the uncertainty associated with the frequency response of the estimated models is proposed. The statistical tool we will resort to is the bootstrap method [ET93, ST95], along the lines of the results in [BL00]. The bootstrap is a computational statistical method which was originally introduced to solve the following problem ([ET93, ST95]): given a random, independent, identically distributed (i.i.d.) sample $x = (x_1, x_2, \ldots, x_n)$ drawn from an unknown distribution F, one computes an estimate $\hat{\theta}$ of the parameter $\theta = t(F) = t[x]$ on the basis of the available data, and would like to assess the accuracy of the obtained estimate, in terms of its standard deviation or its variance.

Various approaches have been proposed to apply the bootstrap for variance estimation in time series analysis ([ST95]), signal processing ([Sha98]) and system identification ([BL00, TL02]).

For the present purposes and with reference to the problem of evaluating the standard deviation for the frequency response of the estimated model, the method of bootstrapping residuals can be synthesized as follows:

1. Estimate the linear model $[\hat{A},\hat{B},\hat{C},\hat{D},\hat{K}]$ from the available input/output data (u,y) and compute the estimate for the points of interest of its frequency response $\hat{G}(j\omega_k)$, $k=1,\ldots,N$.

2. Compute the optimal prediction error for the identified model:

$$e(t)=y(t)-\hat{y}(t). \tag{7}$$

3. Obtain an estimate $\hat{F}_e$ for the distribution F_e of the prediction error. In this work a parametric estimate will be considered and the normality assumption for the distribution of the residual will be made.

4. Generate B replications $(u^{*(i)},y^{*(i)})$, $i=1,\ldots,B$ of the original data set (u,y), with $u^{*(i)}=u$ and $y^{*(i)}$ obtained by feeding the identified model $[\hat{A},\hat{B},\hat{C},\hat{D},\hat{K}]$ with the deterministic input $u^{*(i)}=u$ and the stochastic input $e^{*(i)}$, $i=1,\ldots,B$ where $e^{*(i)}$ is constructed by resampling (with replacement) from the distribution $\hat{F}_e$.

5. Estimate B replications of the identified model and of the points of interest for the frequency response $\hat{G}^{*(i)}(j\omega_k)$, $k=1,\ldots,N$.

6. The estimate of the standard error for the frequency response of the model is finally given by:

$$\hat{\sigma}_{\hat{G}(j\omega_k)}=\frac{1}{\sqrt{B-1}}\Big(\sum_{i=1}^{B}(\hat{G}^{*(i)}(j\omega_k)-\bar{\hat{G}}^{*}(j\omega_k))^2\Big)^{\frac{1}{2}} \tag{8}$$

   where

$$\bar{\hat{G}}^{*}(j\omega_k)=\frac{1}{B}\sum_{i=1}^{B}\hat{G}^{*(i)}(j\omega_k). \tag{9}$$

In a similar way one can obtain estimates of the standard deviation for the poles and zeros of the estimated model.

3 Identification-oriented quadrotor flight testing

The aim of this Section is to provide some information about the experimental set-up used in this study and a description of the identification and validation experiments which have been carried out to characterise the dynamic response of the hovering Mikrokopter. In the following we will refer to the body coordinate frame

attached to the quadrotor and defined according to Figure 1 (the X_B axis is aligned with the longitudinal axis, pointing forward).

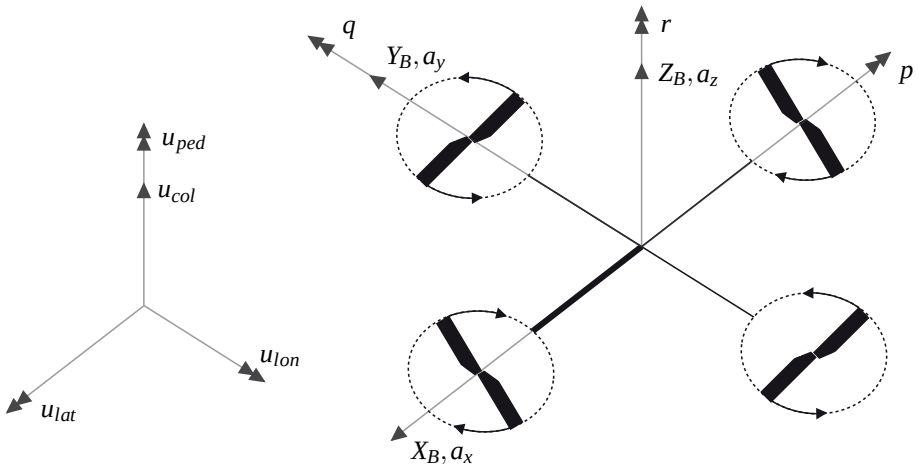

Figure 1: Definition of the control inputs (left) and of the body reference frame and measured outputs (right).

3.1 The experimental setup

The quadrotor used in this work is a modified version of the Mikrokopter platform, an open source project developed and distributed by HiSystems GmbH (Germany). The Mikrokopter consists of a frame composed by four tubes held together by a metal cross as shown in Figure 2, with the four motors placed at the end of the tubes. The onboard electronics are piled up at the centre of the cross in order to maintain a symmetric

Figure 2: The Mikrokopter quadrotor used in this study.

mass distribution. The size of the quadrotor is approximately $45 \times 45 \times 20$ cm and its mass is about 1 kg (with battery). The quadrotor is powered with a Lithium-ion polymer battery (11.1 V, 2200 mAh) that

guarantees an autonomy of about 15 minutes. The original design provides three electronic boards:

Flight-Ctrl It is the main board of the quadrotor. It includes the AVR Atmel 8-bit microcontroller (20 MHz), a set of three MEMS accelerometers and a set of three gyroscopes. This board is the flight controller, indeed it uses the measurements of the sensors and the command inputs taken through the receiver to set the motors speed rates in the proper way. The sensors outputs are sampled using the internal ADC with a 10 bits resolution.

BL-Ctrl (x4) It is the driver of the motor. The microcontroller mounted on this board is an AVR Atmel 8-bit (8MHz) and it is dedicated to the generation of the PWM signal in order to control the motor angular rate according to the set-point communicated through the Inter Integrated Circuit (I^2C) bus by the Flight-Ctrl board. It is able to provide up to 5 A at 15 V.

Navi-Ctrl It is dedicated to record the flight data. This board mounts an AVR Atmel 16-bit microcontroller (25 MHz) and it communicates with the Flight-Ctrl through the Serial Peripherical Interface (*SPI*).

The original firmware has been modified in order to generate input sequences for the identification and to obtain flight data at a sampling frequency of 100 Hz. This data is stored in a microSD card during flight and downloaded for processing after landing.

3.2 Input-output variables selection

In view of identifying a model of the hovering quadrotor for control design, in this paper the variables considered as inputs and outputs are the ones commonly corresponding to control and measured variables in a typical quadrotor control architecture.

Concerning the inputs, quadrotors are mostly (though not exclusively) controlled by varying the angular rates of the four rotors. However, it is well known that the forces and moments generated by the rotors are quadratic functions of the rotors angular rates (see, *e.g.*, [CLD05]), so adopting the rotor angular rates as inputs for the model would entail both a strong nonlinearity in the equations (due to the quadratic dependence) and a strong coupling between the inputs and the response of the individual axes (as the angular rates of the four rotors are always varied simultaneously, regardless of which degree of freedom of the quadrotor is to be controlled). To avoid these difficulties, a change of variables is usually adopted in the literature on quadrotor modelling and control to define control inputs which enter linearly the equations of motion,

namely

$$u = \begin{bmatrix} u_{col} & u_{lon} & u_{lat} & u_{ped} \end{bmatrix}^T = \begin{bmatrix} \Omega_1^2 + \Omega_2^2 + \Omega_3^2 + \Omega_4^2 \\ \Omega_4^2 - \Omega_2^2 \\ \Omega_3^2 - \Omega_1^2 \\ \Omega_2^2 + \Omega_4^2 - \Omega_1^2 - \Omega_3^2 \end{bmatrix},$$

where Ω_i, $i = 1,\ldots,4$ are the angular rates of the four rotors. Up to a scale factor, u_{col} (where *col* stands for collective) can be interpreted as a force along the vertical body axis and is therefore the control input used to control the vertical motion of the quadrotor (see also Figure 1). Similarly, u_{lat}, u_{lon} and u_{ped} can be interpreted as, respectively, a rolling, pitching and yawing moment around the body axes and therefore can be used to control the three attitude degrees of freedom (*lat* standing for lateral, *lon* for longitudinal and *ped* for pedal, in analogy with the rotorcraft literature). Ultimately, u_{lon} and u_{lat} also control the longitudinal and lateral motion of the quadrotor (see, again, Figure 1 and [CLD05] for details).

The output vector, on the other hand, includes the measurements provided by the available inertial sensors, *i.e.*, $y = \begin{bmatrix} a_x & a_y & a_z & p & q & r \end{bmatrix}^T$, where a_x, a_y and a_z are the measurements of the components of the acceleration of the quadrotor along the three body axes and p, q and r are, respectively, the measurements of the components of the quadrotor's angular rate, expressed in the body frame according to the sign conventions depicted in Figure 1.

3.3 Identification experiments

The problem of defining suitable approaches to the experimental testing of a rotorcraft platform has been studied extensively in the literature of piloted rotorcraft, see for example [HK97, TR06]. The key aspect when planning the class of inputs to be applied to the vehicle is the domain in which data will be processed in the identification procedure. Indeed, for frequency-domain approaches such as the ones proposed in [TR06] periodic excitation is desirable (*e.g.*, frequency sweeps, so as to minimise leakage in the computation of frequency spectra). For time-domain identification, on the contrary, this requirement is not necessary so it is possible to employ input sequences which can excite a broad range of frequencies in shorter experiments than swept sines or multi-sines. Concerning the execution of identification experiments in flight, they can be carried out either manually, with the pilot exciting the dynamics of the helicopter using the remote control, or automatically, by implementing on-board functions to generate the input sequences for the experiments. In the case of a small-scale helicopter, manual excitation is not sufficiently fast, so an automatic command generation function has been implemented.

In view of the application of the time-domain identification method described in Section 2, the input sig-

nal adopted for identification experiments is the so-called 3211 piece-wise constant sequence. The numbers used in the designation refer to the relative time intervals between control reversals, see as an example the top part of Figure 3 where a double 3211 sequence is depicted. As discussed in [HK97], this input sequence, developed at the German Aerospace Center DLR for flight dynamics testing, excites a wide frequency band within a short time period, so it is also suited for moderately unstable systems. Guidelines for the design of 3211 sequences can be derived by the analytical computation of the spectrum of the sequence as a function of its duration. Details can be found in, *e.g.*, [KM06], where it is recommended to select the duration of the second (2) step as half the period of the expected dominant mode of the response to be identified. As it is known from prior knowledge and time-domain analysis of open-loop responses that the dominant dynamics of the quadrotor (*i.e.*, the pitch and roll responses) is located in the frequency domain at about 5 rad/s, this guideline led to a choice for the duration of the first (3) step of 0.9 seconds, which is also close to the maximum operable on a quadrotor without it flying too far away from trim. Furthermore, the amplitude of the steps has been chosen to achieve a satisfactory tradeoff between the conflicting requirements of ensuring that attitude changes during the experiments remain limited and of achieving a satisfactory signal-to-noise ratio in the measured outputs. Asymmetry between the amplitude of positive and negative steps has been also introduced, to obtain tests ending with almost null velocity (see the top panel of Figure 3). For the identification phase multiple datasets have been used: three double 3211s (the 3211 maneuver has been repeated to collect more data) for an overall duration of approximately 20 seconds. For the cross-validation phase (*i.e.*, the choice of the model order as well as of the tuning parameters for the identification algorithm) a double 3211 has been used for a duration of approximately 6.5 seconds.

Finally, the input signal used for the validation test is a so-called doublet, *i.e.*, a sequence of two opposite steps of equal duration and amplitude. More precisely, a doublet with a duration of approximately 4 seconds has been used. All the data has been filtered with a lowpass filter with a cutoff frequency of 5 Hz.

It is important to point out that while experiments exciting u_{col} have been carried out in open-loop, the identification of the response to the other control inputs has been carried out using closed-loop data because of the open-loop unstable nature of the platform under study. Note, however, that the identification method considered in this study (see Section 2) can provide unbiased estimates of the dynamics of the system regardless of the input/output correlation introduced by feedback control.

4 Experimental results

4.1 Time-domain data

As an illustrative example of the collected flight data, in Figure 3 the response of the vertical acceleration to a double 3211 applied to u_{col} is shown (the input command is expressed in terms of percentage of the trim value). As can be seen from the time history of the input in Figure 3, the actual input sequence applied

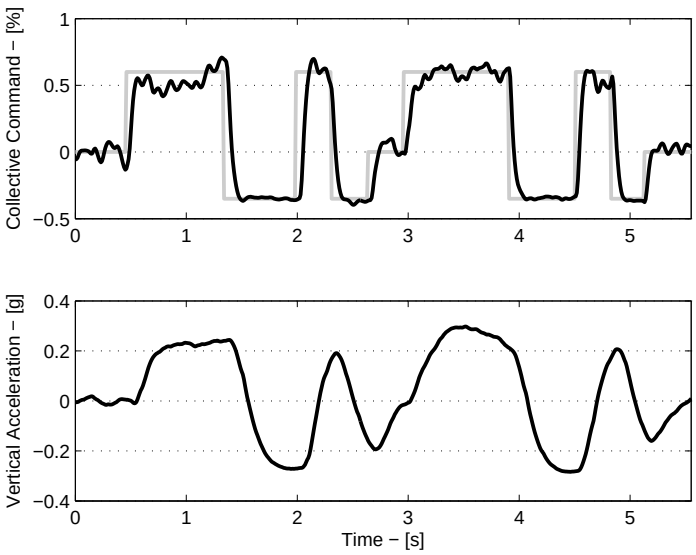

Figure 3: Example of identification data. Top: ideal (grey) and real (black) 3211 collective excitation; bottom: response of vertical acceleration.

by the on-board electronics is not exactly equal to the desired one, still the (double) 3211 profile is clearly visible. Figure 4, on the other hand, shows the time histories of all the measured outputs during the same experiment, to motivate the choice of developing uncoupled models for individual DOFs of the quadrotor. Indeed, it is apparent from the figure that the excitation of u_{col} has a significant effect only on the vertical acceleration, while all the other outputs are essentially unaffected. Similar considerations can be made for the other input variables - the details have been omitted for brevity. Finally, correlation analyses between inputs and outputs have been used to assess the possible presence of delays in the quadrotor's response. Unlike what occurs typically in full scale helicopters, time delays in this case are negligible.

4.2 Identification of uncoupled models for the individual DOFs

Both model order and the tuning parameters of the identification algorithm (*i.e.*, the position of the Laguerre pole a and the parameters of the PBSID$_{opt}$ algorithm) have been selected using a cross-validation approach.

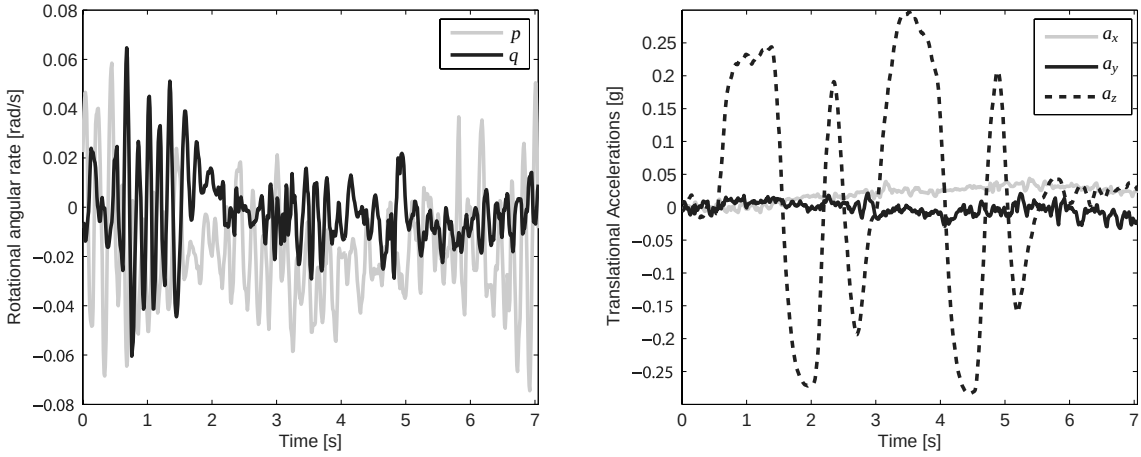

Figure 4: Response of measured variable to 3211 collective excitation. Left: pitch and roll rates; right: acceleration components.

Input	Model order (n)	Laguerre pole (a)
Collective	3	16
Pedal	3	16
Longitudinal	3	21
Lateral	3	15

Table 1: Selected tuning parameters of the algorithm for the identification of each model.

More precisely, as is the case with all SMI algorithms, the choice of model order can be based on the inspection of the singular values of the estimated state sequence for the identified model, while the selection of a and of the parameters of the PBSID$_{opt}$ algorithm has been carried out by checking the norm of the simulation error over the cross-validation dataset. The results of this step are shown in Table 1 for the model order and the position of the Laguerre pole a. Before the validation step, the identified models have been simplified by removing zeros occurring at frequencies well above the excitation bandwidth. For the sake of completeness, the identified models are reported hereafter in equations (10)-(13).

$$G_{col}(s) = \frac{a_z}{u_{col}} = \frac{1.2498(s+0.3451)}{(s+16.49)(s+5.309)(s+1.933)} \tag{10}$$

$$G_{yaw}(s) = \frac{r}{u_{ped}} = \frac{0.077646(s+5.475)(s-0.2086)}{(s+11.03)(s^2+0.2838s+0.06947)} \tag{11}$$

$$G_{lon}(s) = \begin{bmatrix} \frac{q}{u_{lon}} \\ \\ \frac{a_x}{u_{lon}} \end{bmatrix} = \begin{bmatrix} \frac{0.22016(s+0.2579)(s-0.2596)}{(s+1.865)(s^2-1.285s+8.067)} \\ \\ \frac{-0.011659(s-3.271)(s+3.681)}{(s+1.865)(s^2-1.285s+8.067)} \end{bmatrix} \tag{12}$$

$$G_{lat}(s) = \begin{bmatrix} \frac{p}{u_{lat}} \\ \\ \frac{a_y}{u_{lat}} \end{bmatrix} = \begin{bmatrix} \frac{-0.20194(s^2+0.09235s+0.2532)}{(s+1.82)(s^2-1.388s+10.02)} \\ \\ \frac{-0.00359(s-9.182)(s+4.164)}{(s+1.82)(s^2-1.388s+10.02)} \end{bmatrix}. \tag{13}$$

As can be seen from equation (10), the response of the quadrotor on the vertical axis is asymptotically stable and non-oscillatory, being characterised by real poles only. The dominant mode is located at about 2 rad/s, corresponding to a dominant time constant of approximately 0.5 s. Similarly, as can be seen from (11) the response of the yaw rate is also asymptotically stable, but with an oscillatory dominant mode. As expected, on the other hand, the response of the roll and pitch axes is characterised by an unstable, oscillatory mode. Note, in passing, the significant symmetry between the models for lateral and longitudinal response. In particular, the models have the same structure (up to the location of the zeros, on which more comments will be made in subsections 4.4 and 4.5) corresponding to the overall symmetry of the quadrotor platform, which therefore has been successfully captured by the identified models. Small differences in the numerical values of the poles positions can be attributed to asymmetries such as, *e.g.*, different inertial properties due to the mounting of the battery on the quadrotor (aligned with the roll axis, which therefore has a smaller moment of inertia and, accordingly, a slightly faster response, as can be seen by comparing the poles of $G_{lat}(s)$ and $G_{lon}(s)$).

4.3 Time-domain validation

The performance of the identified models has been checked by comparing the simulated outputs with the measured response to a doublet excitation applied on each of the control variables, as discussed in Section 3.3. The results of the validation experiments are presented in Figure 5 for the response of the vertical acceleration to the collective input, Figure 6 for the response of the yaw rate to the pedal input and Figures 7 and 8 for, respectively, the response of the pitch (roll) rate and of the longitudinal (lateral) acceleration to the longitudinal (lateral) input. As for the identification phase, the validation experiments for the response to changes in u_{lat}, u_{lon} and u_{ped} have been carried out in closed-loop.

As can be seen from the figures, the identified models capture the essential features of the response of the quadrotor along all the axes.

Finally, to complete the analysis of the results the bootstrap-based approach to uncertainty analysis summarised in Section 2.3 has been applied to both the frequency responses associated with the transfer functions in equations (10)-(13) and the corresponding positions of poles and zeros in the complex plane. The results are reported in the following subsections.

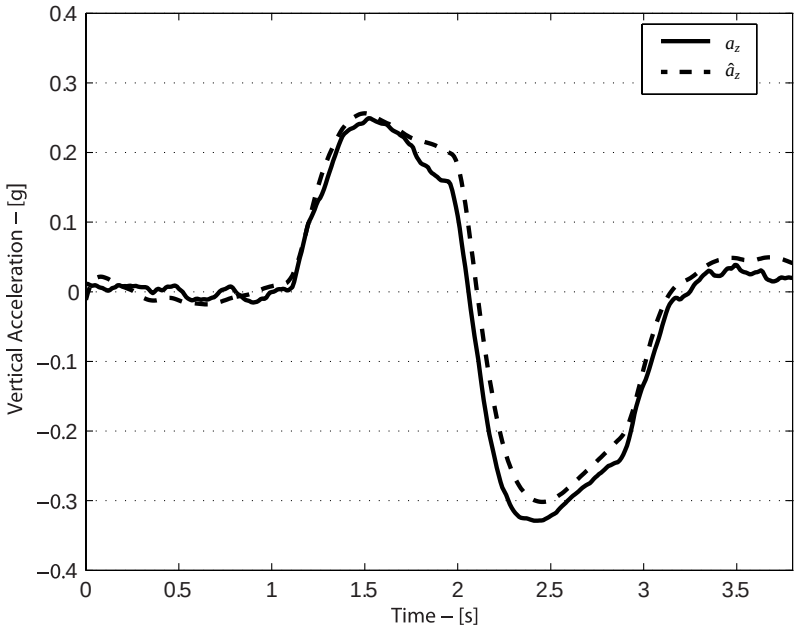

Figure 5: Response of vertical acceleration to collective doublet (measured: solid line; estimated: dashed line).

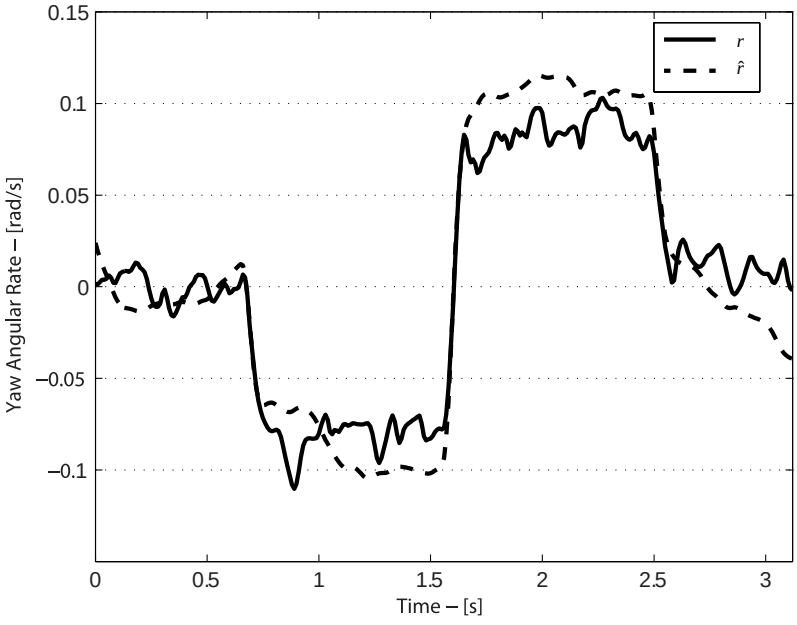

Figure 6: Response of yaw rate to pedal doublet (measured: solid line; estimated: dashed line).

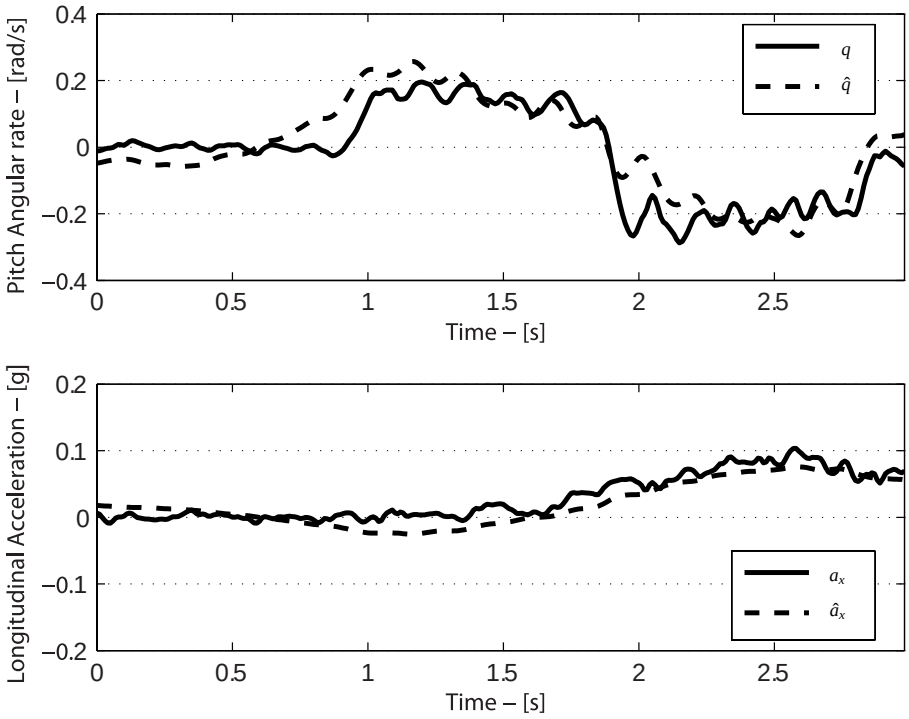

Figure 7: Response of pitch rate (top) and longitudinal acceleration (bottom) to longitudinal cyclic doublet (measured: solid line; estimated: dashed line).

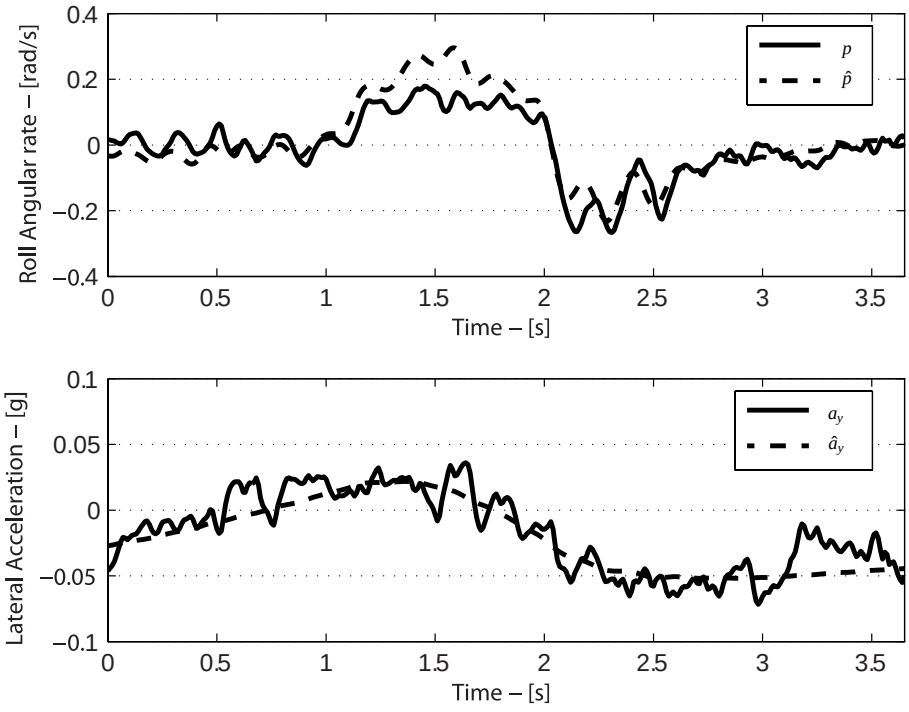

Figure 8: Response of roll rate (top) and lateral acceleration (bottom) to lateral cyclic doublet (measured: solid line; estimated: dashed line).

4.4 Uncertainty analysis: frequency responses

The results of the uncertainty analysis for the frequency responses of the identified models are reported in Figures 9-14, where the frequency responses corresponding to the identified models are compared with 1000 replications computed using the bootstrap.

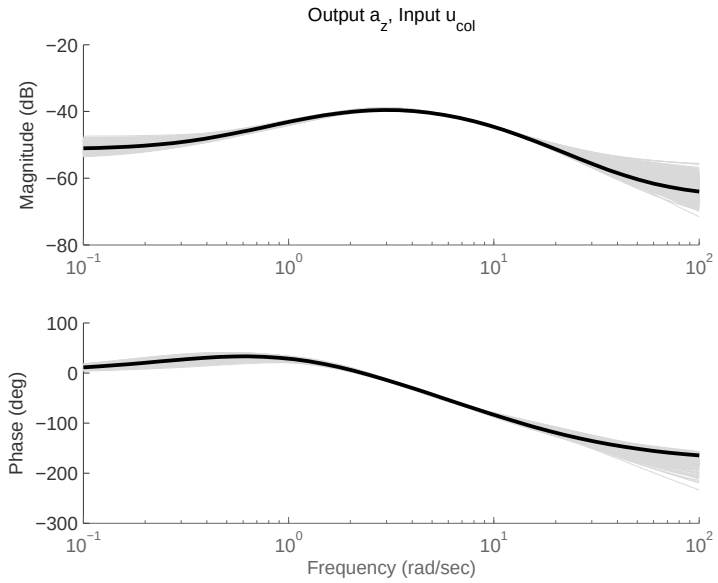

Figure 9: Frequency response of vertical acceleration to collective (black line: nominal model; grey lines: bootstrap replicas).

As can be seen from Figure 9, the response of the vertical axis is captured by the model with very good accuracy, the uncertainty band having a very limited amplitude both in magnitude and phase over the excitation bandwidth (approximately 1-10 rad/s). Clearly some uncertainty is to be expected at low and high frequency, however since for the purpose of controller design what is really relevant is model accuracy around the crossover frequency, this level of model accuracy can be considered adequate. The reader, however, should recall that the response of the vertical axis is asymptotically stable and therefore its identification has been carried out in open-loop.

Uncertainty analysis is particularly informative in the case of unstable models generated from closed-loop data. Indeed, in such a case gathering accurate information about the low frequency response is harder than in open-loop identification, due to both limitations in the duration of the experiments and the low-frequency action of the feedback controller which ”masks” the true dynamics of the open-loop system. As a consequence, one expects significant uncertainty appearing in the low frequency part of the frequency

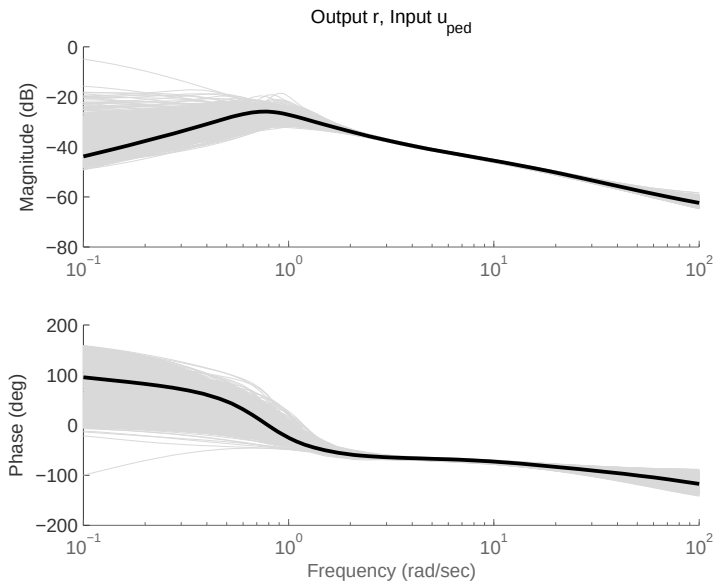

Figure 10: Frequency response of yaw rate to pedal (black line: nominal model; grey lines: bootstrap replicas).

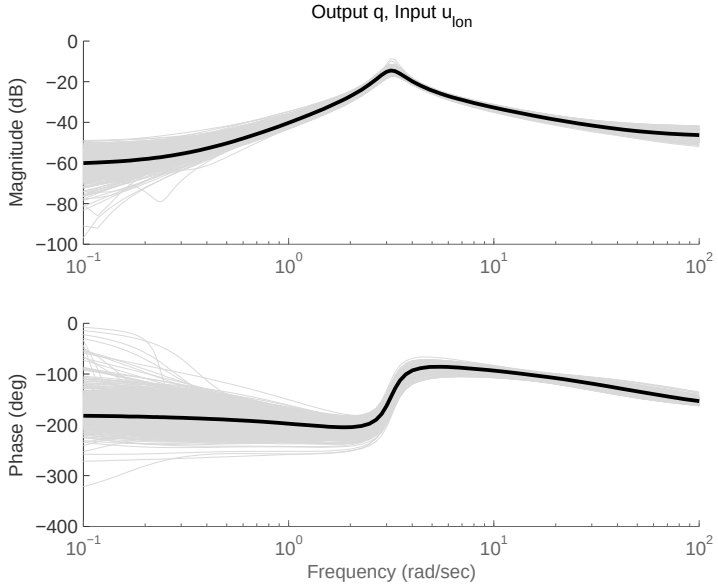

Figure 11: Frequency response of pitch rate to longitudinal cyclic (black line: nominal model; grey lines: bootstrap replicas).

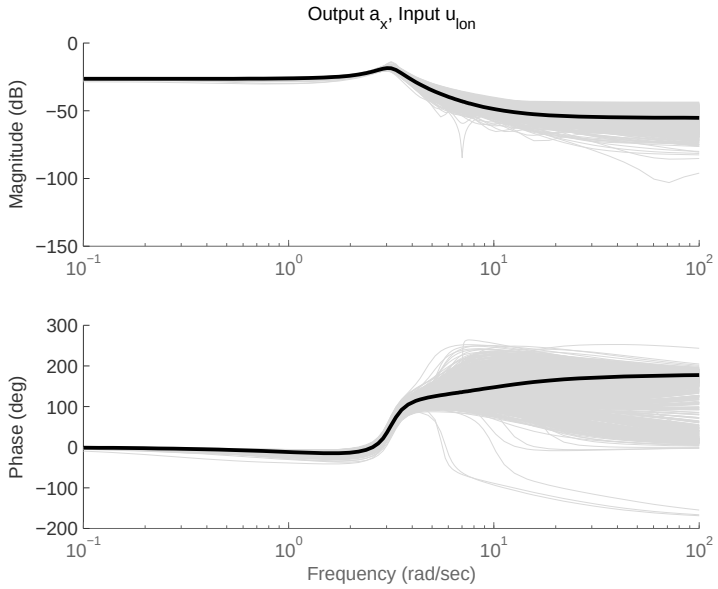

Figure 12: Frequency response of longitudinal acceleration to longitudinal cyclic (black line: nominal model; grey lines: bootstrap replicas).

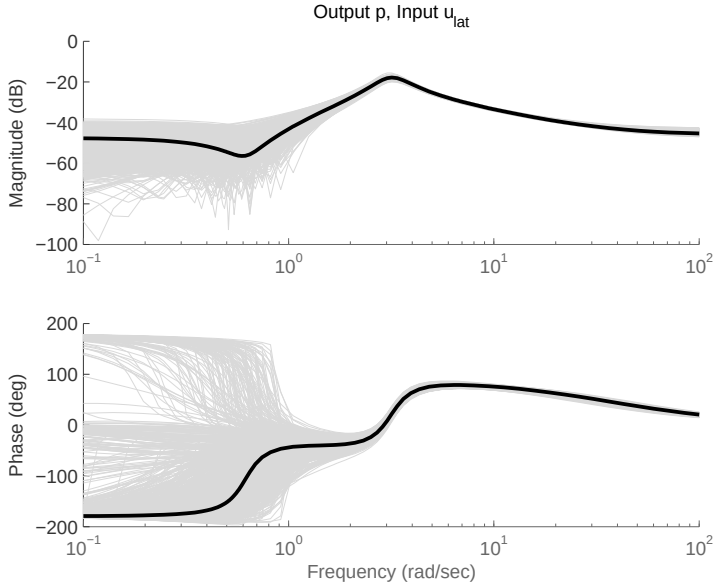

Figure 13: Frequency response of roll rate to lateral cyclic (black line: nominal model; grey lines: bootstrap replicas).

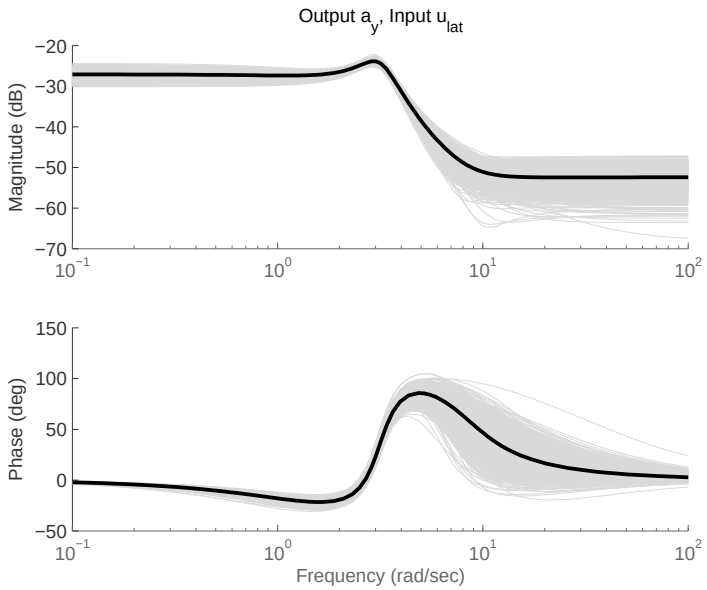

Figure 14: Frequency response of lateral acceleration to lateral cyclic (black line: nominal model; grey lines: bootstrap replicas).

response of the identified model. Fortunately, however, basic insight in the dynamics of the system can be exploited to reduce such uncertainty: for example, if the sign of the gain is known *a priori* in view of the physical interpretation of the control inputs, one can confirm whether the nominal identified model, in spite of the spread of the low-frequency uncertainty, is essentially correct.

This effect is clearly visible in the response of the yaw axis, depicted in Figure 10, which is captured quite accurately by the identified model starting from about 1 rad/s but is not equally accurate at lower frequencies.

Figures 11 and 12 on the other hand represent the frequency responses for the longitudinal response of the quadrotor. In the responses one can readily recognise the unstable complex conjugate poles which dominate the response. In addition, note that in this case the uncertainty associated with the identification procedure is concentrated at low frequency for the response of the pitch rate and at high frequency for the response of the longitudinal acceleration. The lateral response of the quadrotor, reported in Figures 13 and 14, is qualitatively similar to the longitudinal one (again, confirming the essential symmetry of the considered configuration), except for the low frequency behaviour of the roll rate frequency response (Figure 13). Indeed in this case, the low frequency derivative character of the response is captured in the model by means of a complex conjugate pair of zeros, which leads to a significantly different phase curve with respect to the pitch rate one. Note however that even though this portion of the estimated response is

associated with large uncertainty, there is no ambiguity about the sign of the gain of the response, which is known *a priori* from physical considerations and coincides with the one of nominal model. This can be also confirmed by the histogram of the values of the low-frequency phase for the 1000 bootstrapped models, see Figure 15. As can be seen, more than 75% of the models exhibit a phase close enough to -180° to validate

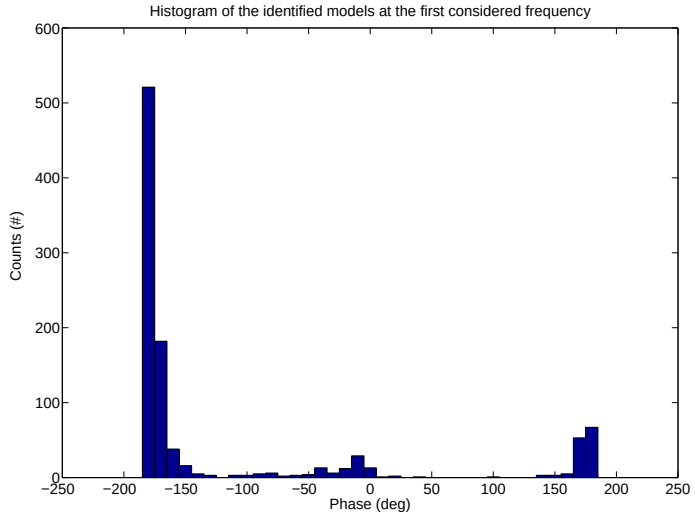

Figure 15: Histogram of the low-frequency phase for the frequency response of the 1000 bootstrapped models of the roll rate.

the prior knowledge of a negative gain. A very small number of bootstrapped models exhibit a phase close to 0°, while less than 10% of the bootstrapped models show an initial phase around $+180^\circ$.Over the excitation bandwidth, however, the identified model appears to be accurate also in this case.

In summary, it can be concluded that the performance of the identified model is adequate for control systems design provided that the control loops are closed within the above mentioned excitation bandwidth. In order to further reduce the residual uncertainty in the models, additional experiments ought to be carried out, trying to maximise the length of the available datasets so as to improve the low frequency content. Note, however, that limited performance in the identification of the low frequency portion of the response is intrinsic in the closed-loop operation during experiments.

4.5 Uncertainty analysis: poles and zeros

A similar analysis, again based on the bootstrap method, can be carried out for the location of poles and zeros of the identified models. Note in particular that for the longitudinal and lateral responses we focus on the zeros of the individual transfer functions rather than on the MIMO ones in view of the fact that conventional

control architectures for quadrotor control would lead to separate loop closures on the individual transfer functions (angular rate for attitude control, acceleration for position control). As is well known, the position of zeros and poles in the complex plane plays a major role in determining the achievable closed-loop performance. In particular, for the case of unstable and/or non-minimum phase systems, the position of right-half plane zeros and poles imposes, respectively, upper and lower bounds to the closed-loop bandwidth (see, *e.g.*, the classical papers [FL85, Ste03]). Along the lines of the previous subsection, the bootstrap method has been applied and 1000 replicas of the identified models have been obtained. For the vertical response of the quadrotor, the results are depicted in Figure 16, where the left panel shows a histogram of the position of the 1000 replicas of the poles, while the right one shows the same results for the zeros. It appears that all the 1000 replicated models remain asymptotically stable and the two dominant poles (nominal locations at -1.933 and -5.309) are estimated with a very low uncertainty, while the "fast" pole located in the nominal model at -16.49 has a much more significant uncertainty associated with it (again, not surprising as its location is above the excited bandwidth). Similarly, the zero of the transfer function appears to be estimated very accurately and, most importantly, remains minimum phase for all the bootstrapped replicas. For the response of the yaw axis, in Figure 17 the histograms for the natural frequencies and the damping

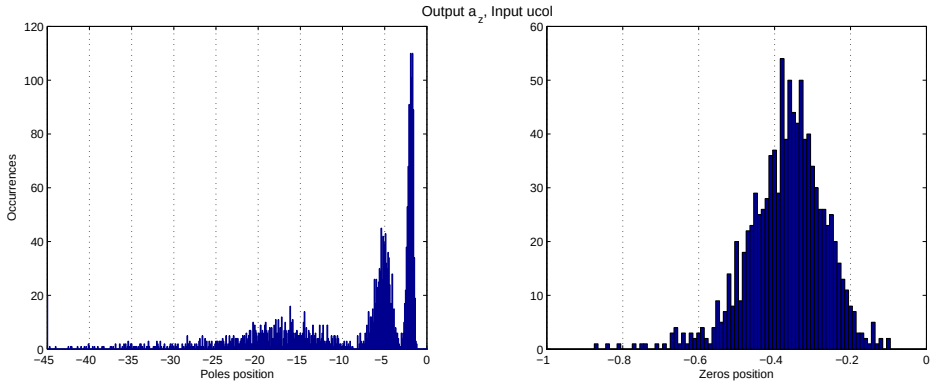

Figure 16: Histograms of poles (left) and zero (right) of the transfer function from collective to vertical acceleration.

factors of the poles are depicted, while the zeros are illustrated in Figure 18. Concerning the poles, the peaks in the histograms associated with the complex conjugate poles and the real pole are clearly visible; again, the dominant complex conjugate mode is captured with small dispersion, while the faster real pole is determined with larger uncertainty. As for the zeros, it is interesting to note that the (low frequency) non-minimum phase one is actually characterised by an uncertainty range which lies across the imaginary

axis, which reflects the high level of uncertainty in the phase response of the yaw rate apparent from Figure 10.

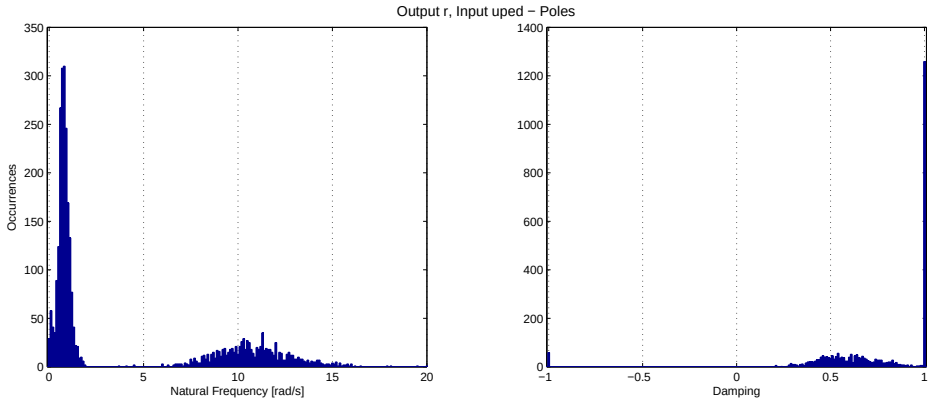

Figure 17: Histograms of poles of the transfer function from pedal to yaw rate. Left: natural frequencies; right: damping factors.

Finally, the results for the response of the longitudinal axis are presented (the lateral response is omitted for brevity) in Figures 19-20 (poles) and 21 (zeros). Concerning the poles, it appears form Figure 19 that the dominant, unstable complex conjugate mode is identified with great accuracy, while there is some uncertainty associated with the real pole, for which a histogram is presented in Figure 20. The natural frequency of the unstable mode, which can be placed at 2.84 rad/s therefore provides information about the minimum bandwidth for the control of the longitudinal response. As for the zeros of the two transfer functions associated with the longitudinal axis, Figure 21 clearly shows the non-minimum phase of the responses, confirming also in a statistical sense the characteristics of the identified model. Note in particular that the estimation of the right-half plane zeros is quite accurate.

5 Concluding remarks

The problem of black-box model identification of the dynamics of a quadrotor helicopter has been considered. In view of the open-loop instability of the quadrotor, closed-loop experiments have been carried out and a continuous-time subspace model identification approach capable of dealing with such experimental conditions has been adopted. Furthermore, a complete analysis of the uncertainty associated with the identified model has been performed, using tools from the field of computational statistics. The results of the study show that the considered approach is an effective one as far as the characterisation of the local dynamics of the quadrotor is concerned and can also provide useful uncertainty information for the pur-

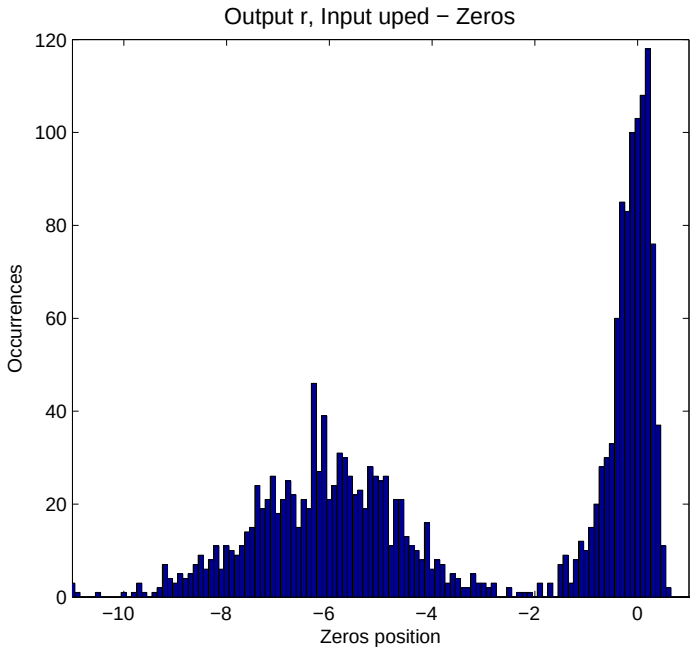

Figure 18: Histogram of zeros of the transfer function from pedal to yaw rate.

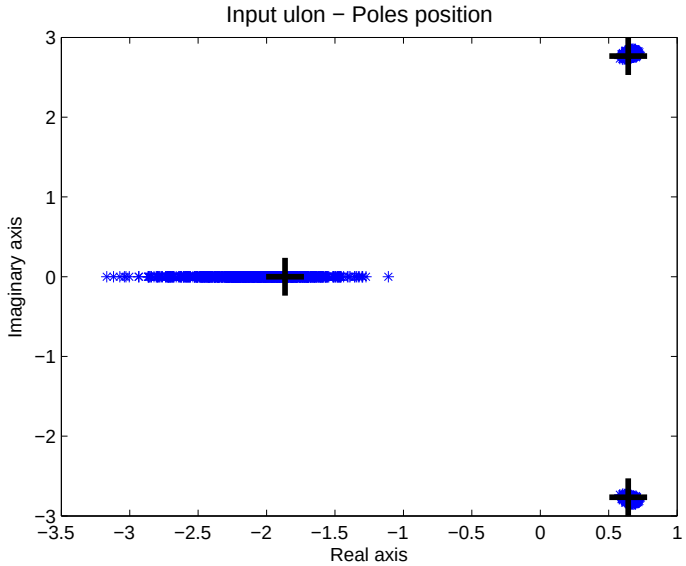

Figure 19: Poles of the transfer functions from longitudinal control to pitch rate and longitudinal acceleration.

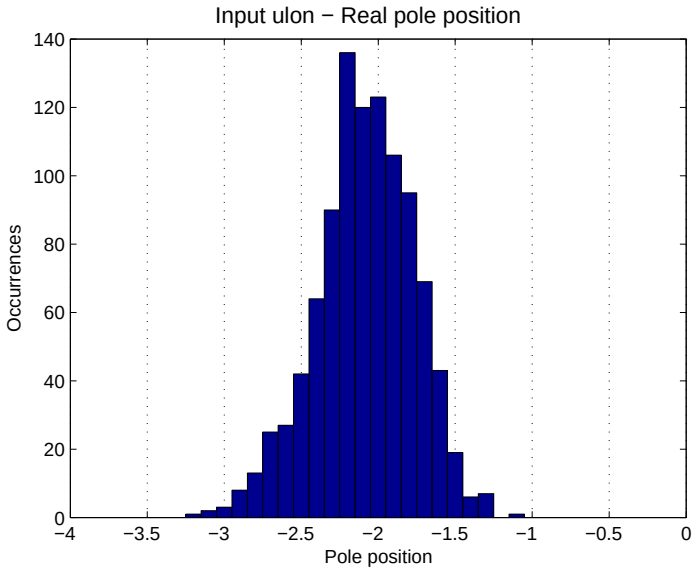

Figure 20: Histogram of real pole of the transfer functions from longitudinal control to pitch rate and longitudinal acceleration.

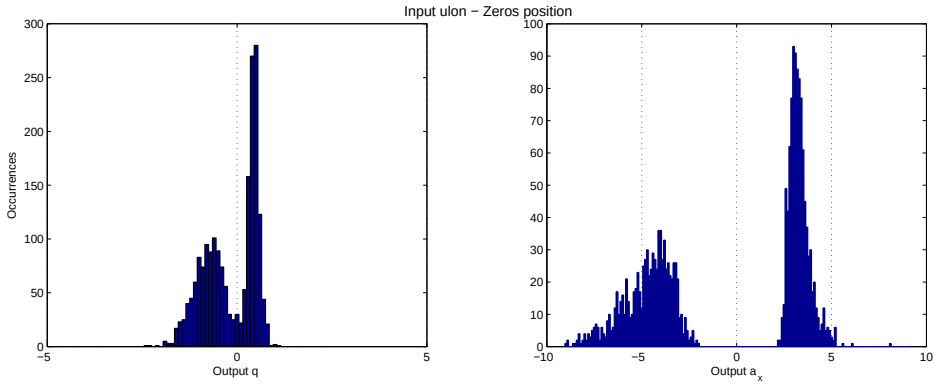

Figure 21: Histogram of zeros of the transfer functions from longitudinal control to pitch rate (left) and longitudinal acceleration (right).

pose of robust control system design, both in the frequency domain and in the time domain. Future work will deal with the problem of optimising the input sequences used in the identification experiments (some preliminary results are available in [BBL11]), which in turn will allow the analysis of the platform in more general flight conditions, and to consider additional sensors in the model identification.

References

[BBL11] F. Beltramini, M. Bergamasco, and M. Lovera. Experiment design for MIMO model identification, with application to rotorcraft dynamics. In *IFAC World Congress, Milano, Italy*, 2011.

[BBS07] S. Bouabdallah, M. Becker, and R. Siegwart. Autonomous miniature flying robots: coming soon! *IEEE Robotics & Automation Magazine*, 14(3):88–98, 2007.

[BL97] S. Bittanti and M. Lovera. Identification of linear models for a hovering helicopter rotor. In *Proceedings of the 11th IFAC Symposium on system identification, Fukuoka, Japan*, 1997.

[BL00] S. Bittanti and M. Lovera. Bootstrap-based estimates of uncertainty in subspace identification methods. *Automatica*, 36(11):1605–1615, 2000.

[BL11a] M. Bergamasco and M. Lovera. Continuous-time predictor-based subspace identification for helicopter dynamics. In *37th European Rotorcraft Forum, Gallarate, Italy*, 2011.

[BL11b] M. Bergamasco and M. Lovera. Continuous-time predictor-based subspace identification using Laguerre filters. *IET Control Theory and Applications*, 5(7):856–867, 2011. Special issue on Continuous-time Model Identification.

[Chi07] A. Chiuso. The role of autoregressive modeling in predictor-based subspace identification. *Automatica*, 43(3):1034–1048, 2007.

[CLD05] P. Castillo, R. Lozano, and A.E. Dzul. *Modelling and control of mini-flying machines*. Springer-Verlag New York Inc, 2005.

[CP05] A. Chiuso and G. Picci. Consistency analysis of certain closed-loop subspace identification methods. *Automatica*, 41(3):377–391, 2005.

[CV97] C.T. Chou and M. Verhaegen. Subspace algorithms for the identification of multivariable dynamic error-in-variables state space models. *Automatica*, 33(10):1857–1869, 1997.

[DMB06] L. Derafa, T. Madani, and A. Benallegue. Dynamic modelling and experimental identification of four rotors helicopter parameters. In *IEEE International Conference on Industrial Technology*, pages 1834–1839. IEEE, 2006.

[DSL09] A. Das, K. Subbarao, and F. Lewis. Dynamic inversion with zero-dynamics stabilisation for quadrotor control. *IET Control Theory & Applications*, 3(3):303–314, 2009.

[ET93] B. Efron and R. Tibshirani. *An introduction to the bootstrap*. Chapman and Hall, 1993.

[FL85] J. Freudenberg and D. Looze. Right half plane poles and zeros and design tradeoffs in feedback systems. *IEEE Transactions on Automatic Control*, 30(6):555–565, 1985.

[Hav01] B. R. J. Haverkamp. *State space identification: theory and practice*. PhD thesis, Delft University of Technology, 2001.

[HDQ05] B. Huang, S.X. Ding, and S.J. Qin. Closed-loop subspace identification: an orthogonal projection approach. *Journal of Process Control*, 15(1):53–66, 2005.

[HK97] P. Hamel and J. Kaletka. Advances in rotorcraft system identification. *Progress in Aerospace Sciences*, 33(3-4):259–284, 1997.

[HMLO02] T. Hamel, R. Mahony, R. Lozano, and J. Ostrowski. Dynamic modelling and configuration stabilisation for an X4-flyer. In *IFAC World Congress, Barcelona, Spain*, 2002.

[HOBM08] G. Heredia, A. Ollero, M. Bejar, and R. Mahtani. Sensor and actuator fault detection in small autonomous helicopters. *Mechatronics*, 18(2):90–99, 2008.

[Jat06] R. Jategaonkar. *Flight Vehicle System Identification*. AIAA, 2006.

[JVC99] R. Johansson, M. Verhaegen, and C.T. Chou. Stochastic theory of continuous-time state-space identification. *IEEE Transactions on Signal Processing*, 47(1):41–51, 1999.

[KCL06] B. Kim, Y. Chang, and M. Hyung Lee. System identification and 6-DOF hovering controller design of unmanned model helicopter. *JSME International Journal Series C Mechanical Systems, Machine Elements and Manufacturing*, 49(4):1048–1057, 2006.

[KM06] V. Klein and E.A. Morelli. *Aircraft System Identification: Theory And Practice*. AIAA, 2006.

[KO10] Y. Kinoshita and Y. Ohta. Continuous-time system identification using compactly supported filter kernels generated from Laguerre basis functions. In *49th IEEE Conference on Decision and Control, Atlanta, USA*, 2010.

[KT04] S. K. Kim and D. Tilbury. Mathematical modeling and experimental identification of an unmanned helicopter robot with flybar dynamics. *Journal of Robotic Systems*, 21(3):95–116, 2004.

[LCMK02] M. La Civita, W. Messner, and T. Kanade. Modelling of small-scale helicopters with integrated first-principles ans system identification techniques. In *Proceedings of the 58th American Helicopter Society Annual Forum*, 2002.

[LI11] P. Li and Postlethwaite I. Subspace and bootstrap-based techniques for helicopter model identification. *Journal of the American Helicopter Society*, 56(1):012002, 2011.

[LM96] L. Ljung and T. McKelvey. Subspace identification from closed loop data. *Signal Processing*, 52(2):209–215, 1996.

[Lov03] M. Lovera. Identification of MIMO state space models for helicopter dynamics. In *13th IFAC Symposium on System Identification, Rotterdam, The Nederlands*, 2003.

[MK12] R. Mahony and V. Kumar. Aerial robotics and the quadrotor [from the guest editors]. *IEEE Robotics & Automation Magazine*, 19(3):19–19, 2012.

[MOGG08] G. Mercère, R. Ouvrard, M. Gilson, and H. Garnier. Identification de systèmes multivariables à temps continu par approche des sous-espaces. *Journal Européen des Systèmes Automatisés*, 42(2-3):261–285, 2008.

[Oht05] Y. Ohta. Realization of input-output maps using generalized orthonormal basis functions. *Systems & Control Letters*, 22(6):437–444, 2005.

[Oht11a] Y. Ohta. Stochastic system transformation using generalized orthonormal basis functions with applications to continuous-time system identification. *Automatica*, 47(5):1001–1006, 2011.

[Oht11b] Y. Ohta. System transformation of unstable systems induced by a shift-invariant subspace. In *50th IEEE Conference on Systems and Control, Orlando, USA*, 2011.

[OK04] Y. Ohta and T. Kawai. Continuous-time subspace system identification using generalized orthonormal basis functions. In *16th International Symposium on Mathematical Theory of Networks and Systems, Leuven, Belgium*, 2004.

[OKY02] A. Ohsumi, K. Kameyama, and K. I. Yamagushi. Subspace identification for continuous-time stochastic systems via distribution-based approach. *Automatica*, 38(1):63–79, 2002.

[PM09] P. Pounds and R. Mahony. Design principles of large quadrotors for practical applications. In *IEEE International Conference on Robotics and Automation, Kobe, Japan*, 2009.

[SBL12] M. Sguanci, M. Bergamasco, and M. Lovera. Continuous-time model identification for rotorcraft dynamics. In *16th IFAC Symposium on System Identification, Brussels, Belgium*, 2012. Submitted.

[Sha98] S. Shamsunder. Signal processing applications of the bootstrap. *IEEE Signal Processing Magazine*, 15:38, 1998.

[ST95] J. Shao and D. Tu. *The jackknife and bootstrap*. Springer, 1995.

[Ste03] G. Stein. Respect the unstable. *IEEE Control Systems*, 23(4):12–25, 2003.

[TL02] F. Tjarnstrom and L. Ljung. Using the bootstrap to estimate the variance in the case of undermodeling. *IEEE Transactions on Automatic Control*, 47(2):395–398, 2002.

[TR06] M. Tischler and R. Remple. *Aircraft And Rotorcraft System Identification: Engineering Methods With Flight-test Examples*. AIAA, 2006.

[Ver94] M. Verhaegen. Identification of the deterministic part of MIMO state space models given in innovations form from input-output data. *Automatica*, 30(1):61–74, 1994.

[VODM96] P. Van Overschee and B. De Moor. *Subspace identification: theory, implementation, application*. Kluwer Academic Publishers, 1996.

[VV94] M. Verhaegen and A. Varga. Some experience with the MOESP class of subspace model identification methods in identifying the BO105 helicopter. Technical Report TR R165-94, DLR, 1994.

[VV07] M. Verhaegen and V. Verdult. *Filtering and System Identification: A Least Squares Approach*. Cambridge University Press, 2007.